Extended Abstracts of the 22nd (1990 International) Conference on Solid State Devices and Materials, Sendai, 1990, pp. 139-142

Efficient Coupling of Monte Carlo and Drift Diffusion Method with Applications to MOSFETs

Hans KOSINA, Siegfried SELBERHERR

Institute for Microelectronics
Technical University of Vienna, Gußhausstraße 27-29
A-1040 Vienna, Austria

A new method for coupling Monte Carlo (MC) and Drift Diffusion (DD) model has been developed. The space dependent parameters mobility and thermal voltage occuring in the DD-equation are calculated by means of MC. Their definitions, which are general and therefore not restricted to simple band structure models, are derived from the Boltzmann transport equation (BTE). With this method regional MC analysis can be performed - just in the high field region of a device mobility and thermal voltage have to be calculated by MC, thus including non-local effects such as velocity overshoot and ballistic transport, whereas in low field regions local models are sufficient.

1. INTRODUCTION

In the active region of a submicron device, the electric field is often very high and undergoes rapid changes over a small distance. In this situation, the widely used Drift Diffusion model becomes inadequate, while the Monte Carlo method being based on accurate physical models is well suited to be applied. For description of low field transport, however, the DD model which uses local transport coefficients provides sufficient accuracy. Moreover, the DD model has turned out to be even superior to the MC method in regions with retarding fields. Therefore several attempts were published to combine the DD- and MC technique in order to benefit from the different capabilities of both methods [1] [2].

2. TRANSPORT THEORY

Assuming the BTE to be valid, multiplication with wave vector component k_i and integration over $\mathbf{k}$ leads to the equation for the first moment, which reads for electrons

$$-q\left(E_i+\frac{1}{qn}\sum_{j=1}^{2}\frac{\partial(n<\hbar k_i\, v_j>)}{\partial x_j}\right)=$$

$$<\int(\hbar k_i-\hbar k_i')\,S(\mathbf{k},\mathbf{k}')\,d^3\mathbf{k}'>\,,\quad i=1,2 \qquad (1)$$

where E denotes the electric field, n the electron concentration and v the the group velocity. The average operator $<A>$ is the mean value of $A(\mathbf{k})$ weighted by the local distribution function $f(\mathbf{x},\mathbf{k})$. The left hand side can be interpreted as driving force that acts on the electron ensemble, consisting of electric field plus diffusion term, whereas the right hand side describes the rate of momentum loss due to scatterings. This equation stating momentum balance can be expressed in a form similar to the DD current relation. The parameters needed for this current relation are derived in the following way. For band structures with spheric and ellipsoidal energy surfaces the vector valued momentum loss integral is colinear with the momentum $\hbar\mathbf{k}$

$$\int(\hbar\mathbf{k}-\hbar\mathbf{k}')S(\mathbf{k},\mathbf{k}')d^3\mathbf{k}' = \hbar\mathbf{k}\,\lambda_m(E)\,. \qquad (2)$$

Here the proportionality factor $\lambda_m(E)$ is the momentum scattering rate. With the local average velocity and the local momentum loss mobility can be defined as

$$\mu = q\,\frac{\|<\mathbf{v}>\|}{\|<\hbar\mathbf{k}\,\lambda_m(E)>\|}\,. \qquad (3)$$

This definition does not rely on the relaxation time approximation and, since no effective mass occurs in this formula, extension to general bands is straight forward. In the latter case μ would become a ten-

sor. The definition of the thermal voltage tensor (which is proportional to the temperature tensor $U_{ij} = \frac{k_B}{q} T_{ij}$) results directly from the momentum conservation equation (1)

$$U_{ij} = \frac{1}{q} < \hbar k_i \, v_j > . \quad (4)$$

This definition is again independent of the underlying band structure model. Inserting these definitions in equation (1) we obtain a general current relation

$$J_i = q \, n \, \mu \left(E_i + \frac{1}{n} \sum_{j=1}^{2} \frac{\partial (n U_{ij})}{\partial x_j} \right) . \quad (5)$$

The differences between this current relation and the classical one are twofold. Firstly, the diffusion term is obviously more complicated. But if the assumption of diagonal form of the thermal voltage tensor is justified the sum disappears and, from the point of view of device simulation programs, this current relation can be implemented in a conventional simulator by doing only a few modifications. Secondly, the parameters μ and U_{ij} can no longer be treated simply as parameters depending on electric field or other local quantities, as it is usually done in the conventional DD model, because they carry information of the local distribution function. By means of the MC method, which is a tool to solve the BTE in a stochastical way, we evaluate these parameters. The conventional simulator using the MC parameters $\mu(\mathbf{x})$ and $U_{ij}(\mathbf{x})$ in the current relation (5) is then capable of recovering the MC results for $n(\mathbf{x})$ and $\mathbf{J}_n(\mathbf{x})$. In this way hot electron effects playing an important role in submicron devices, such as velocity overshoot and hot carrier diffusion, are consistently included in the conventional simulator. The solution is performed globally in the whole device, but only in the high field region mobility- and temperature profiles have to be extracted from the MC procedure. In regions with low fields and low spatial inhomogenities local models can be used thus saving computation time. It shall be noted that this coupling method is justified rigorously from the BTE [1].

3. THE SEMICONDUCTOR MODEL

For the conduction band of silicon we use a model consisting of six anisotropic valleys with a first order correction for nonparabolicity [4]. Acoustic intravalley scattering in the elastic approximation, intervalley phonon scattering, surface roughness scattering and coulomb scattering are taken into account. Except of the latter one all mechanisms are isotropic. In the case of surface scattering in the inversion layer the wave vector is redistributed randomly in a plane parallel to the $Si-SiO_2$ interface [3]. For isotropic scattering mechanisms the momentum scattering rate does not differ from the total scattering rate. The following superposition implies independence of all scattering processes

$$\lambda_m(E) = \lambda_{ac}^{tot} + \lambda_{opt}^{tot} + \lambda_{surf}^{tot} + \lambda_{ion}^{m} . \quad (6)$$

Coulomb interaction is the only one to be treated separately. We evaluate the momentum loss integral (2) with the Brooks-Herring formulation for the transition rate $S(\mathbf{k}, \mathbf{k}')$ and obtain

$$\lambda_{ion}^{m}(E) = \lambda_{ion}^{tot}(E) - \lambda_{ion}'(E) . \quad (7)$$

The subtraction corresponds to the difference of initial and final wave vector in (2). In the following notation β is the reciprocal screening length.

$$E_\beta = \frac{\hbar^2 \beta^2}{2 m_d} , \qquad \xi = \frac{2k^2}{\beta^2} .$$

Introducing further shorthands

$$C_{ion} = \frac{N_I \, q^4}{2^{3/2} \pi \epsilon^2 \sqrt{m_d}}, \qquad \gamma(E) = E(1 + \alpha E),$$

the two terms at the right hand side of (7) can be written as

$$\lambda_{ion}^{tot} = \frac{C_{ion}}{E_\beta^2} \sqrt{\gamma} \, (1 + 2\alpha E) \frac{1}{1 + 2\xi}$$

$$\lambda_{ion}' = \frac{C_{ion}}{8 \gamma^2} \sqrt{\gamma} \, (1 + 2\alpha E) \Big(2\xi \frac{1 + \xi}{1 + 2\xi} - ln(1 + 2\xi) \Big) .$$

Fig.1 depicts the energy dependencies of total (λ_{ion}^{tot}) and momentum (λ_{ion}^{m}) scattering rate for ionized impurities, and additionally the total scattering rates for acoustic intravalley phonons λ_{ac} and one representative intervalley phonon mode (emission and absorption).

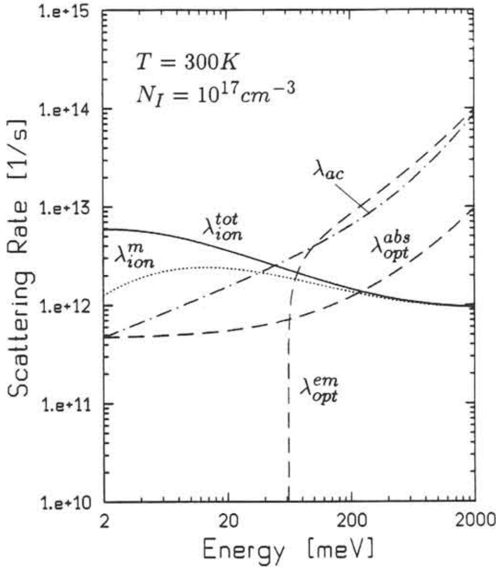

Fig. 1. Total and momentum scattering rates used for mobility calculation

4. RESULTS

An n-channel MOSFET with $L_{gate} = 0.25\mu m$, $t_{ox} = 5nm$ was simulated at room temperature using the combined technique. The device has a metallurgical channel length of $L_{eff} = 0.15\mu m$ and exhibits a threshold voltage $U_t = 0.23V$.

For practical simulation of a MOSFET, electrons are injected in source, where they fully thermalize before entering the channel. In the region of interest, usually near drain, a sufficiently large number of particles is supplied by a particle split algorithm as proposed in [5], thus reducing the statistical uncertainty of the results. The potential distribution in the device was calculated with MINIMOS [6] under a bias condition of $U_{GS} = U_{DS} = 2.5V$ and $U_{BS} = 0V$.

The effect of carrier heating in bulk silicon which is present in the MC model is shown in *fig.2*. As can be expected the temperature component built up from the velocity and wave vector components parallel to the field is larger than that one built up from components normal to the field. The scalar temperature resulting from the average energy rises steeper at high fields than the temperatures actually needed to describe transport. Two dimensional temperature profiles in the area near drain are depicted in *fig.3*. The lateral temperature T_{xx} has a maximum value at the surface, while the maximum of T_{yy} is shifted away from surface. Degradation due to hot electron injection into the oxide can be more accurately modeled by using the spatial distribution of T_{yy} than by using the scalar temperature obtained from average energy. In our simulations the off-diagonal temperatures never exceeded 15% of the main-diagonal elements. Thus we estimate their contributions to the driving force to be of minor importance and assume diagonal form ($T_{ij} = T_{ij}\delta_{ij}$) in the current relation (5).

Comparing *fig.4* and *fig.5* we see that the large normal field within the inversion layer (*fig.4*) does not appear in the driving force (*fig.5*). This is obvious since the normal field is compensated by diffusion. The electric field in the source junction (*fig.4*) is compensated by diffusion as well, since in this area the driving force calculated by MC vanishes. The field peak near the drain edge however appears almost unchanged in the driving force, thus accelerating and heating up the electron gas in this area.

Velocity of electrons in the channel is plotted in *fig.6*. The effective channel extends from $0.05\mu m$ to $0.2\ \mu m$, the positions of the junctions of source and drain subdiffusion, respectively. In the first half of this range the surface velocity (curve A) is lower than the velocities within the inversion layer since the electrons are pressed towards the surface. Near drain the pressing force has opposite direction and the electron velocity is maximal at the surface. The field peak near drain induces a velocity overshoot of 90% related to the bulk saturation velocity. Comparison of *fig.4* and *fig.5* showed that in the overshoot region diffusion is not important. Therefore velocity overshoot is treated in this model more like a drift phenomenon. It is reproduced by the DD current relation (3) by incorporting the nonlocal mobility.

REFERENCES

1) S.Bandyopadhyay; IEEE Trans.ED.34(1987) 392.
2) Y.J.Park; IEEE Trans.ED.31 (1984) 1724.
3) C.Hao; Sol.State.El.28 (1985) 733.
4) C.Jacoboni; Rev.Mod.Phys.55 (1983) 645.
5) A.Phillips; Appl.Phys.Lett.30 (1977) 528.
6) W.Hänsch; IEEE Trans.ED.34 (1987) 1074.

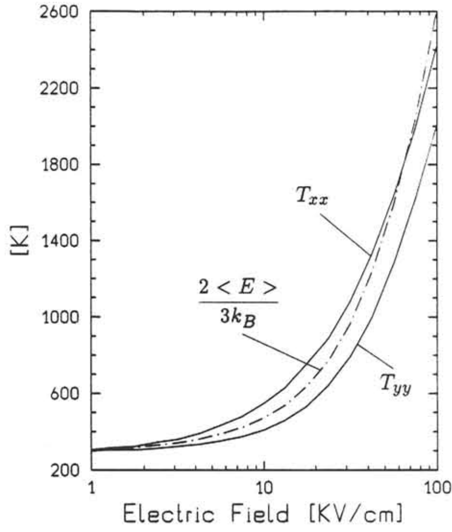

Fig. 2. Temperatures parallel (T_{xx}) and normal (T_{yy}) to the electric field in comparison with a scalar temperature obtained from the average electron energy.

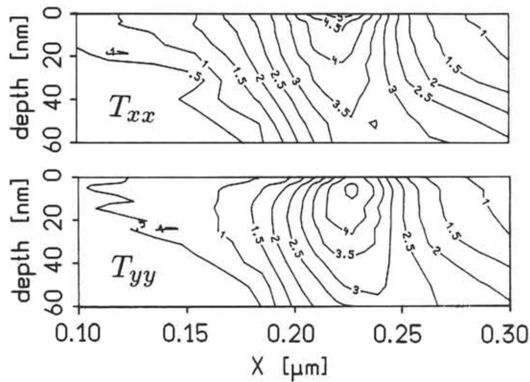

Fig. 3. Lateral and transversal electron temperatures in a quarter micron MOSFET (units [1000 K]).

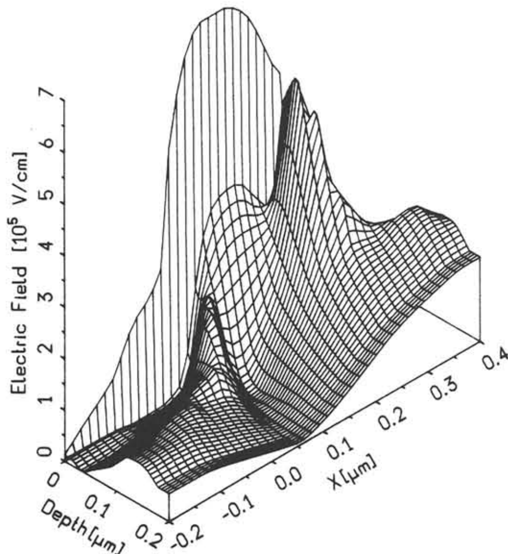

Fig. 4. Electric field in the same device.

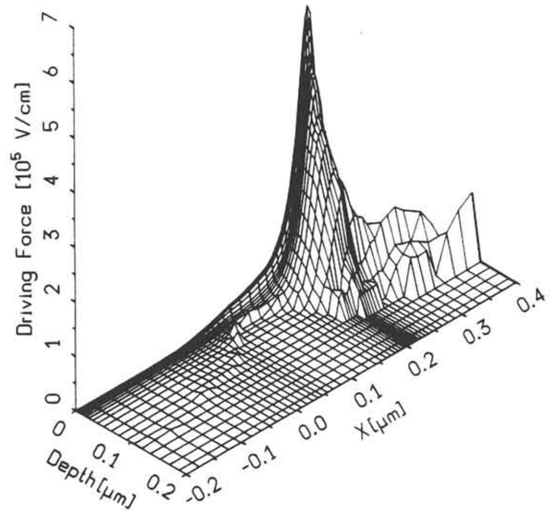

Fig. 5. Driving force in the same device calculated by MC.

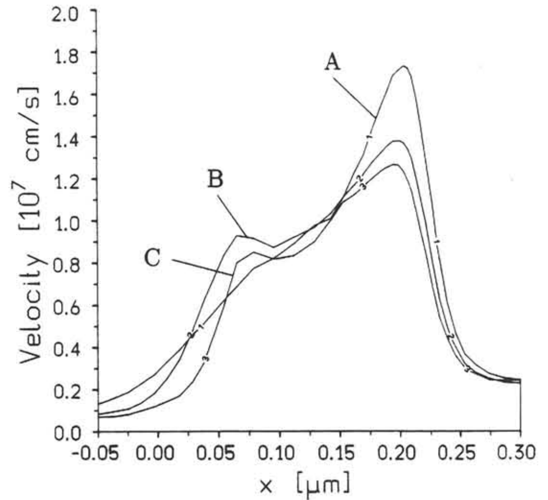

Fig. 6. Electron average velocity along the channel. Curve A: at the Si–SiO_2 interface. Curves B and C: 5 nm and 10nm away from interface.